N-Cadherin Association with Lipid Rafts Regulates Its Dynamic Assembly at Cell-Cell Junctions in C2C12 Myoblasts

Marie Causeret,*† Nicolas Taulet,*† Franck Comunale,* Cyril Favard,‡§ and Cécile Gauthier-Rouvière*

*Centre de Recherches de Biochimie Macromoléculaire, Centre National de la Recherche Scientifique Formation de Recherche en Evolution 2593, 34293 Montpellier, France; and ‡Institut de Physique de la Matière Complexe, Centre National de la Recherche Scientifique, Sophia-Antipolis, 06560 Valbonne, France

Cadherins are homophilic cell-cell adhesion molecules implicated in cell growth, differentiation, and organization into tissues during embryonic development. They accumulate at cell-cell contact sites and act as adhesion-activated signaling receptors. Here, we show that the dynamic assembly of N-cadherin at cell-cell contacts involves lipid rafts. In C2C12 myoblasts, immunofluorescence and biochemical experiments demonstrate that N-cadherin present at cell-cell contacts is colocalized with lipid rafts. Disruption of lipid rafts leads to the inhibition of cell-cell adhesion and disorganization of N-cadherin–dependent cell-cell contacts without modifying the association of N-cadherin with catenins and its availability at the plasma membrane. Fluorescent recovery after photobleaching experiments demonstrate that at the dorsal plasma membrane, lipid rafts are not directly involved in the diffusional mobility of N-cadherin. In contrast, at cell-cell junctions N-cadherin association with lipid rafts allows its stabilization enabling the formation of a functional adhesive complex. We show that lipid rafts, as homophilic interaction and F-actin association, stabilize cadherin-dependent adhesive complexes. Homophilic interactions and F-actin association of N-cadherin are both required for its association to lipid rafts. We thus identify lipid rafts as new regulators of cadherin-mediated cell adhesion.

INTRODUCTION

Cadherins are integral membrane proteins that act as adhesion-activated signaling receptors, playing essential roles in cell recognition and tissues morphogenesis. They promote calcium-dependent homophilic cell-cell adhesion through their extracellular domains. Cadherin cytoplasmic domains bind to catenins, which provide sites of attachment to the actin cytoskeleton and give rise to a functional cadherin complexe (Nagafuchi and Takeichi, 1988). Cadherin is directly associated with β-catenin, γ-catenin, and p120 catenin. The two first proteins interact with α-catenin, which link the cadherin complexe with the actin cytoskeleton. Formation of adherens junctions is a multistep process. Cadherin–catenin complexes initially assemble in the endoplasmic reticulum or the Golgi compartment (Chen *et al.*, 1999; Wahl *et al.*, 2003). They are then transported to the plasma membrane (PM) via a microtubule-dependent kinesin-driven mechanism (Mary *et al.*, 2002; Chen *et al.*, 2003). At the initial stage of adherens junction formation, cadherin–catenin complexes are free to diffuse in the cell membrane before the initiation of the adhesion process and then become anchored to the actin cytoskeleton as a result of their homophilic ligand-triggered recruitment (Sako *et al.*, 1998; Lambert *et al.*, 2002).

Plasma membrane contains cholesterol/sphingolipid-enriched microdomains that dynamically organize specific membrane proteins (Jacobson *et al.*, 1995). These microdomains are found mainly in plasma membrane, but they also form in internal membrane compartments, such as the endocytotic pathway or the Golgi apparatus (Gkantiragas *et al.*, 2001). They can be isolated biochemically by their insolubility in nonionic detergents, such as Triton X-100 at low temperature. The resulting detergent-insoluble glycolipid-rich complexes (DIGs), also called detergent-resistant membranes (DRMs), can be isolated by flotation in sucrose gradients (Iwabuchi *et al.*, 1998). DRMs fall into two main subclasses, noncaveolae and caveolae lipid rafts (Harder and Simons, 1997; Kurzchalia and Parton, 1999). Caveolae are the only morphologically identifiable type of lipid domain and have been recognized as stable flask-like invaginations of the plasma membrane. Lipid rafts are presumed to be too small and transient to be directly observed in cells, making their study difficult and controversial (Kusumi *et al.*, 2004). Proteins found in lipid rafts include glycosylphosphatidylinositol (GPI)-anchored proteins; doubly acylated proteins, such as src; and transmembrane proteins, such as growth factor receptors and adhesion molecules (Niethammer *et al.*, 2002; Roepstorff *et al.*, 2002). The function of lipid rafts could be to select and concentrate molecules in a microenvironment of the membrane to facilitate signal transduction or protein import and trafficking (Simons and Toomre, 2000). Because lateral organization of the cell surface might control

cadherin function, we have analyzed whether N-cadherin is present in lipid raft membrane subcompartments in C2C12 myoblasts. We observed that a fraction of N-cadherin is associated with lipid rafts. Various approaches were used to localize the lipid raft-associated pool of N-cadherin showing that this takes place mainly at cell-cell contact sites. Analysis in living cells of the mobile fraction and lateral diffusion of a N-cadherin (Ncad)/green fluorescent protein (GFP) chimera by fluorescent recovery after photobleaching (FRAP) shows for the first time that N-cadherin association to lipid rafts is required for the establishment of a functional cadherin adhesive complex.

MATERIALS AND METHODS

Drug Treatment and Immunocytochemistry

C2C12 myoblasts were cultured as described previously (Charrasse et al., 2002). Cells were fixed for 5 min in 4% paraformaldehyde (in phosphate-buffered saline [PBS]) followed by a 2-min permeabilization in 0.1% Triton X-100 (in PBS) or in 0.1% saponin (in PBS) for cholera toxin (CTX) and filipin staining (Sigma-Aldrich, St. Louis, MO). Alternatively, cells were incubated in 1% Triton X-100 in 10 mM PIPES, pH 6.8, 50 mM NaCl, 3 mM MgCl$_2$, 300 mM sucrose, and 1 mM phenylmethylsulfonyl fluoride for 1–5 min at 4°C, fixed in 4% paraformaldehyde (in PBS), and stained for N-cadherin or catenins. Monoclonal antibodies to N-cadherin; β-, γ-, and p120 catenins; and caveolin were from BD Transduction Laboratories (Lexington, KY). Rabbit polyclonal anti-α-catenin was from Santa Cruz Biotechnology (Tebu, France). Secondary antibodies were Alexa Fluor 546- or Alexa Fluor 488-conjugated goat anti-mouse antibody (Molecular Probes, Eugene, OR). Biotinylated cholera toxin B subunit (CTX-B) was revealed using Texas Red-conjugated streptavidin (Interchim, Lyon, France).

Cells were treated with methyl-β-cyclodextrin (4 mM MCD for 6 h; Sigma-Aldrich) or cholesterol oxidase (CO) (1 U/ml for 1 or 2 h, Calbiochem, San Diego, CA) in culture medium containing 10% delipidized serum (Sigma-Aldrich). Cytochalasin B (CY) was used at 2 μM for 1 h.

Isolation of DRM Fractions

Four 10-cm dishes of C2C12 were collected by centrifugation, and the cell pellet was resuspended in ice-cooled lysis buffer containing 1% Triton X-100 and fractionated on a 4-ml sucrose gradient (Iwabuchi et al., 1998). Ten fractions were collected from the top, and the protein amount in each fraction was analyzed using bicinchoninic acid assay. Thirty microliters of each fraction was analyzed by SDS-PAGE or by immunoblotting for caveolin; N-cadherin; α-, β-, γ-, and p120 catenins; and β1-integrin (all from BD Transduction Laboratories). Alternatively, isolation of DRM was performed from cell fraction enriched in plasma membranes. Twenty 10-cm dishes of contacting or 50 14-cm dishes of isolated C2C12 myoblasts were processed as described for preparation of fractions enriched in plasma membranes (Gauthier-Rouviere et al., 1998). Scanned autoradiographs were quantified using Aïda/2D densitometry software.

Cell Aggregation Assay

Control, CO-, MCD-, or EGTA-treated cells were dissociated in 0.2 mM EDTA in PBS during 5 min at 4°C to preserve cadherin molecules. Cells were resuspended as single-cell suspensions, and 10^5 cells were placed on each well of a 96-well plate and allowed to aggregate for 30 min in the presence of similar drug treatment. Then, 1% glutaraldehyde was added and images were recorded using a Leica microscope equipped with a 10× phase-contrast objective. The number of cells and aggregates was measured with MetaMorph software, and the percentage of aggregation calculated as (N0 − Nt)/N0 × 100, where Nt is the total aggregate number after the incubation time t and N0 is the total cell number.

Ganglioside GM1 Patching

C2C12 myoblasts were transfected with N-cadherin/GFP, GPI/GFP (gift from B. Nichols, MCR, Cambridge, United Kingdom), NrCAM/GFP (gift from C. Faivre-Sarrailh, Centre National de la Recherche Scientifique, Marseille, France), or myc-tagged transferrin receptor (TfR) (gift by M. Cormont, Institut National de la Santé et de la Recherche, Nice, France) by jetPEI (Qbiogen, Carlsbad, CA). Twenty-four hours later, cells were incubated on ice for 30 min with rhodamine-labeled CTX-B followed by incubation with anti-CTX-B antibody as described previously (Janes et al., 1999). Cells were then fixed in 3% paraformaldehyde in PBS for 15 min, mounted, and analyzed by immunofluorescence. For TfR detection, cells fixed and permeabilized with 0.1% NP-40/phosphate-buffered saline for 2 min and incubated with a mouse monoclonal anti-myc antibody (9E10) followed by incubation with Alexa 488-conjugated anti-mouse antibody (1:2000 dilution; Molecular Probes and Interchim).

Cell Surface Biotinylation

Cell surface proteins were biotinylated by incubating the cells with 1.5 mg/ml sulfo-NHS-SS-biotin (Pierce Chemical, Rockford, IL) as described previously (Le et al., 1999). Cleared lysate (except 20 μl corresponding to the total fraction) was incubated with streptavidin beads (Pierce Chemical) to collect biotinylated proteins. The samples were then analyzed by immunoblotting for N-cadherin. Alternatively, after cell surface biotinylation, cells were processed for DRM isolation. Fractions 3–5 (lipid rafts, LRs) and 8–10 (nonlipid rafts, NLRs) were pooled and incubated with streptavidin beads and processed as described above. Scanned autoradiographs were quantified using Aïda/2D densitometry software.

Immunoprecipitation

Cells were lysed as described previously (Charrasse et al., 2002). Extracts were immunoprecipitated using anti-N-cadherin antibody, and processed as described previously (Mary et al., 2002).

Image Analysis

Images were captured and deconvolved as described previously (Mary et al., 2002). Restored stacks were processed with Imaris (Imagic Bilderverarbeitung, Switzerland), for visualization and colocalization analysis.

Fluorescence Recovery after Photobleaching

Lateral diffusion coefficients (D) and the mobile fractions (M) were measured by FRAP by using the Zeiss LSM Meta 510 confocal microscope. FRAP recoveries were acquired at 37°C on Ncad/GFP-expressing cells plated on glass coverslips, treated or not with CO or CY. The 488-nm line of the Ar+ laser was used for the excitation of GFP. Cells were observed using a 40× water immersion objective (1.2 numerical aperture) with a pinhole adjustment resulting in a 0.9-μm optical slice (1 airy unit). After 20 prebleach scans (1 scan/s), a region of interest (ROI) with a radius w = 1 μm was bleached, and fluorescence recovery was sampled for 4 min, once every second. Bleaching time length was carefully adjusted to be less than one-fifth of the $t_{1/2}$ to achieve correct determination of D. Determination of w was made by FRAP experiments on dipalmitoyl phosphatidylcholine (DPPC): 7-nitrobenz-2-oxa-1,3-diazol-4-yl-phosphatidylcholine (NBD-PC) [99:1 (mol:mol)] multilamellar lipid vesicles at 25°C by using the above-described recording sequence. Because this temperature is low below the melting temperature (T$_m$) of DPPC, no diffusion of NBD-PC could be seen during the experiment, allowing therefore direct measurement of the waist on the image. Experimental recoveries were normalized and corrected for cell z-position fluctuation by using another ROI as an internal standard. Half-recovery times ($t_{1/2}$) and mobile fractions (M) were determined by fitting the normalized recovery curves using a 10th order limited development of a modified equation given in Axelrod et al. (1976) with Origin 6.0 Software. D were then calculated using the equation D = βw^2/4$t_{1/2}$. The paired Student's t test was used for statistical analysis.

RESULTS

N-Cadherin and Catenins Are Present in Lipid Rafts

To analyze whether N-cadherin and catenins are found in lipid raft microdomains in C2C12 myoblasts, we analyzed Triton X-100 lysates in sucrose density gradients. Resistance to solubilization by Triton X-100 at 4°C and light buoyant density have been widely used as a basis for isolating raft membranes, also called DIGs or DRMs (Simons and Ikonen, 1997; Iwabuchi et al., 1998). Analysis of the protein profile of the gradient shows that almost all the proteins were in fractions 8–10 and correspond to detergent-soluble protein (Figure 1A). Few proteins retain their association with lipids and are recovered in DRMs. This is the case for caveolin, the structural components of PM invaginations termed caveolae (Kurzchalia and Parton, 1999), frequently used as a lipid raft marker and that we found enriched in fractions 2–5 (Figure 1A). Western blot analysis showed that a low but significant and reproducible amount of N-cadherin and catenins sedimented in the lipid raft fractions (Figure 1B). A large pool of N-cadherin and catenins was found in the Triton-soluble high-density fractions. Similar data were obtained using Brij 98, a detergent that obviates the problem of modification of membrane phase behavior by chilling (Drevot et al., 2002;
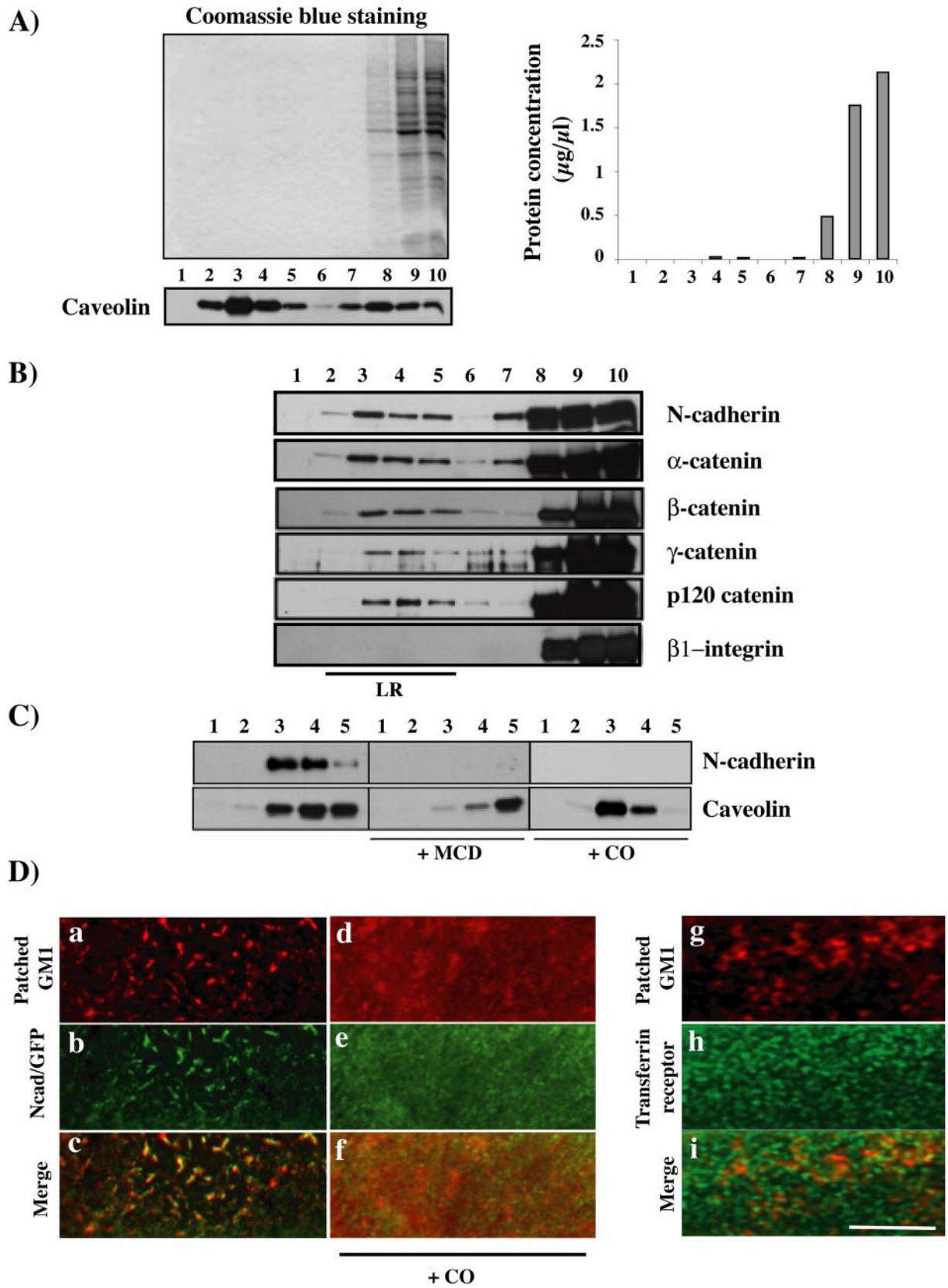
A)

Coomassie blue staining

B)

N-cadherin
α-catenin
β-catenin
γ-catenin
p120 catenin
β1–integrin

LR

C)

N-cadherin
Caveolin

+ MCD   + CO

D)

Figure 1.

Figure 2. N-cadherin associates with lipid rafts at cell-cell contacts. (A) Fractions enriched in plasma membranes obtained from contacting cells were fractionated on sucrose gradients. Each fraction (30 μl) was analyzed for N-cadherin and caveolin distribution by immunoblotting. (B) C2C12 myoblasts were surface biotinylated and fractionated on sucrose gradients. Fractions 3–5 (corresponding to LR fractions) and fractions 8–10 (corresponding to NLR fractions) were pooled, and biotinylated N-cadherin was analyzed by precipitation with streptavidin beads and immunoblotting. (C) Fractions enriched in plasma membranes obtained from isolated cells were fractionated on sucrose gradients. Each fraction (30 μl) was analyzed for N-cadherin and caveolin distribution by immunoblotting.
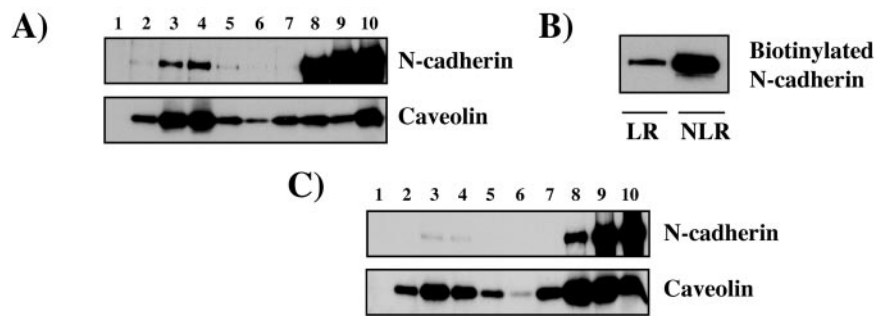
our unpublished data). We analyzed the effects of lipid raft disruption by cholesterol depletion or oxidation through addition of MCD or CO, respectively, on N-cadherin association to DRMs by using sucrose gradients (Smart and Anderson, 2002). MCD or CO addition impairs N-cadherin association to DRMs (Figure 1C), without effect on the amount of N-cadherin found in the detergent-soluble fraction (our unpublished data). The amount of caveolin found in DRMs also decreased, albeit not completely eliminated as reported previously (Ilangumaran and Hoessli, 1998). To further demonstrate the association of N-cadherin in rafts, we used a technique based on the lateral cross-linking of the raft-associated ganglioside GM1 (Harder *et al.*, 1998). Patching of GM1 with the CTX-B subunit and antibodies against CTX-B resulted in copatching of N-cadherin/GFP (Figure 1D, a–c). The copatching with CTX-B of two DRM-associated constructs, GPI-GFP and NrCAM-GFP, was observed, whereas transferrin receptor or β1-integrin were segregated from CTX-B (data not shown, except for transferrin receptor in Figure 1D, g–i). Addition of CO prevented the copatching of N-cadherin with GM1 (d–f). Similar data were obtained using MCD (our unpublished data). These data show that a pool of N-cadherin is associated with lipid rafts.

N-Cadherin and Catenins Associate with Lipid Rafts at Cell-Cell Contact Sites

To analyze the localization of the N-cadherin and catenins associated with lipid rafts, we first studied N-cadherin association to DRMs by using sucrose gradients prepared from enriched plasma membrane preparations (Figure 2A). A fraction of the N-cadherin in the plasma membrane is found associated with lipid rafts (visible in lanes 3 and 4). To further confirm that a pool of N-cadherin in the plasma membrane is associated with lipid rafts, we monitored plasma membrane-associated N-cadherin by cell surface biotinylation at 4°C. Biotinylated cells were lysed with cool Triton X-100 and analyzed on a sucrose gradient. Biotinylated N-cadherin was analyzed in pooled fractions 3–5 (corresponding to LR fractions) and pooled fractions 8–10 (corresponding to NLR fractions) (Figure 2B). This experiment confirms that a fraction of N-cadherin at the plasma membrane is associated with lipid rafts. This fraction is estimated to 16%. We next analyzed N-cadherin association to DRMs by using sucrose gradients prepared from enriched plasma membrane preparations of isolated cells. (Figure 2C). The fraction of N-cadherin found associated with lipid rafts is very low and almost undetectable in this condition (compare Figure 2A, estimated ~16%, and C, estimated ~1%). We also stained cells with either the CTX-B, which binds to GM1 an accepted raft marker, or filipin, an antibiotic that binds to cholesterol that is highly present in rafts (Smart and Anderson, 2002). N-cadherin and CTX-B colocalized at cell-cell junctions (Figure 3A, a–c, arrow), as did N-cadherin and filipin (d–f, arrow). No clear colocalization between N-cadherin and caveolin, a protein marker of caveolae, was detectable at the cell junction (g–i, arrow with asterisk). N-cadherin also codistributed with caveolin in the perinuclear region corresponding to the Golgi apparatus (i, arrowhead). The codistribution of the lipid raft marker CTX-B with N-cadherin or catenins was further analyzed at cell-cell contacts. Image stacks were deconvolved using the Huygens System image restoration software as described in the *Materials and Methods*. Respective colocalization of CTX-B, N-cadherin, and catenin fluorescence was studied using the Imaris colocalization module. As shown in Figure 3B, CTX-B colocalized with N-cadherin and catenins at cell-cell junctions. We can thus propose that N-cadherin and catenins at cell-cell contacts codistribute with a highly enriched lipid raft zone. We then used an additional approach to identify the localization of N-cadherin and catenins within lipid rafts based on the resistance to solubilization in nonionic detergent. Cells were extracted with cold 1% Triton X-100 before fixation and labeling for N-cadherin. As shown in Figure 3C, the insoluble pool of N-cadherin corresponded to the protein located at the cell-cell contacts (b). CO addition strongly decreased the insoluble pool of N-cadherin located at the cell-cell contacts (c). Similar data were obtained with catenins (our unpublished data). Together, these data indicate that N-cadherin is associated with lipid rafts, mainly at cell-cell contacts.

Figure 1 (facing page). N-cadherin and catenins associate with lipid rafts. (A) C2C12 myoblasts were lysed in 1% Triton X-100 and fractionated on a sucrose gradient as described in *Materials and Methods*. Thirty microliters of each fraction were resolved on SDS-PAGE gels and stained with Coomassie Blue. The protein content of each fraction and caveolin distribution along the gradient were analyzed. (B) The distribution of N-cadherin; α-, β-, γ-, and p120 catenins; and β1-integrin in each fraction (30 μl) were analyzed by immunoblotting with the appropriate antibody. (C) C2C12 myoblasts, treated with either MCD, CO, or mock treated, were fractionated on sucrose gradients. Lipid raft fractions (corresponding to 20 μl from fraction from 1 to 5) were analyzed for N-cadherin and caveolin distribution by immunoblotting. (D) GM1 in CO or mock-treated cells was labeled with rhodamine-conjugated cholera toxin B subunit and subsequently patched by the addition of secondary antibody (a and d). Distribution of N-cadherin/GFP (b and e) or transferrin receptor alone (h) or merge with the patched GM1 (c, f, and i) are shown. Bar, 10 μm.
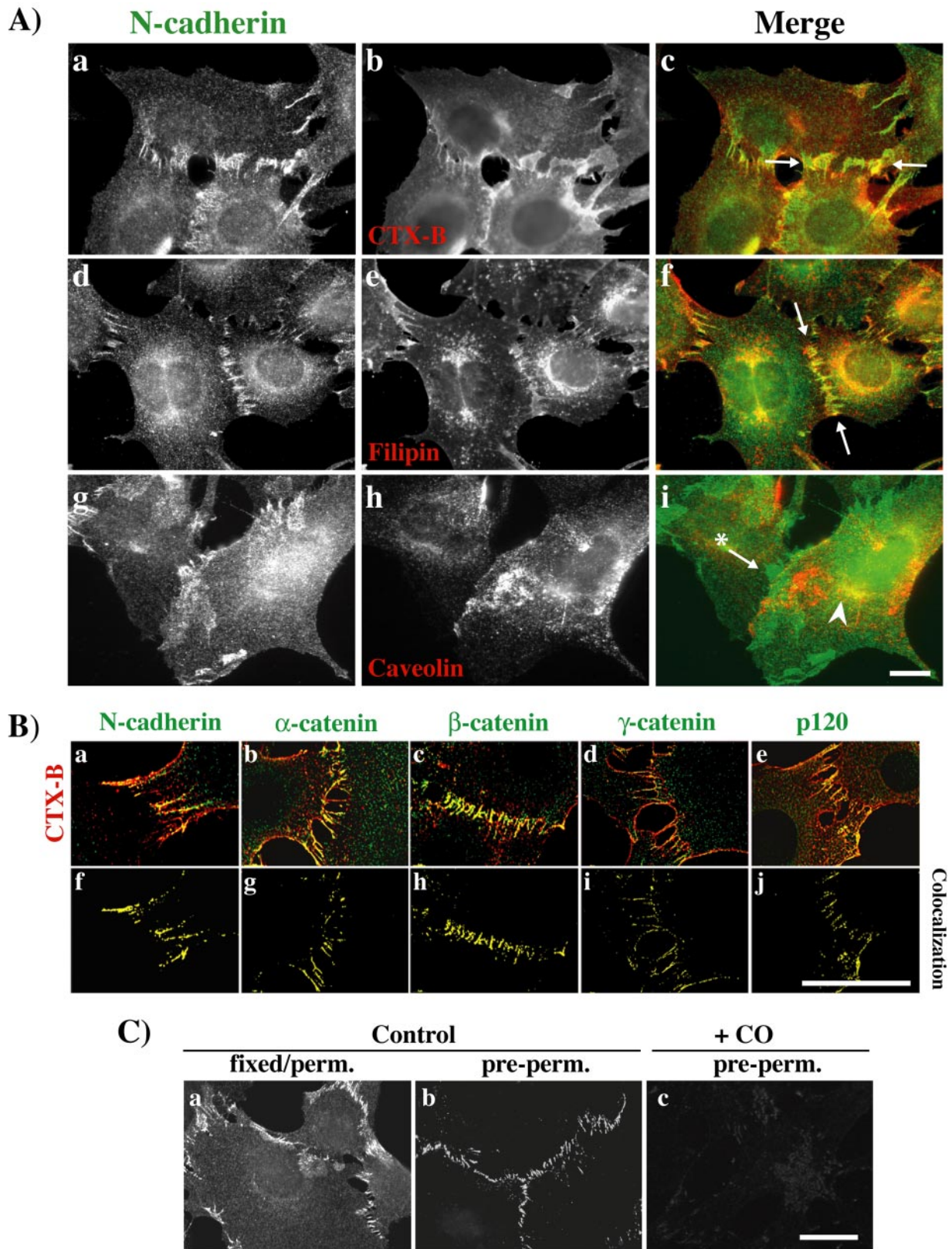
Figure 3. N-cadherin and catenins associate with lipid rafts at cell-cell contacts. (A) C2C12 myoblasts were analyzed by immunocytochemistry and wide-field microscopy for colocalization of endogenous N-cadherin with CTX-B (a–c), filipin (d–f), and caveolin (g–i). Bar, 10 μm. (B) C2C12 myoblasts stained with CTX-B (red in a–e) and with antibodies against N-cadherin (green in a), α-catenin (green in b), β-catenin (green in c), γ-catenin (green in d), and p120 (green in e). Shown are confocal sections crossing the cell-cell contacts. f to j show the colocalization obtained using the Imaris colocalization module. Bar, 10 μm. (C) Control (a and b) or CO-treated (c) C2C12 myoblasts were fixed either before (a) or after (b and c) extraction with cold 1% Triton X-100 and stained with an antibody against N-cadherin. Bar, 10 μm.

Lipid Rafts Disruption Affects N-Cadherin Accumulation at Cell-Cell Contacts

We then studied the effects of lipid raft disruption by cholesterol depletion or oxidation on cell-cell adhesion by using an aggregation assay. Aggregation of C2C12 myoblast was decreased after CO or MCD addition (Figure 4A). Similar effect was obtained after EGTA addition, which chelates extracellular Ca^{2+} and perturbs homophilic interaction. We also analyzed the effects of lipid raft disruption on N-cadherin localization at cell-cell contacts. N-cadherin and CTX-B distribution was analyzed after incubation with MCD or CO (Figure 4B). As previously shown, N-cadherin and CTX-B colocalized at cell-cell junctions (a–c), but MCD or CO addition disrupted N-cadherin accumulation at cell-cell contacts and colocalization with CTX-B (d–f and j–l). Addition of cholesterol-containing culture medium restored N-cadherin association at cell-cell contacts and colocalization with CTX-B (g–i and m–o). To analyze whether CO treatment affects the association of N-cadherin with catenins, we performed coimmunoprecipitation experiments (Figure 4C). We next used a biotinylation assay to specifically analyze N-cadherin at the plasma membrane (Figure 4D). Neither the association of N-cadherin with catenins nor the level of N-cadherin at the cell surface was affected by CO treatment. Similar results were obtained using MCD (our unpublished data). Our data are partially based on results using cholesterol-depleting drugs and notably corroborate results obtained by other approaches. Together, these data argue for a role of lipid rafts in the N-cadherin accumulation at cell-cell contacts, although the results from cholesterol depletion must be interpreted with caution.

Lipid Rafts Stabilize Cadherin-dependent Adhesive Complexes at Cell-Cell Junctions

To analyze whether disruption of lipid rafts affects the assembly dynamics of N-cadherin at cell-cell contacts, we performed FRAP experiments and measured the D and M values of Ncad/GFP in living C2C12 myoblasts. Because N-cadherin was previously shown to be transported and endocytosed through a vesicular mechanism (Le *et al.*, 1999; Mary *et al.*, 2002; Chen *et al.*, 2003), we first controlled whether the fluorescence recovery was only due to the lateral diffusion of Ncad/GFP in the plasma membrane by measuring the fluorescence recovery from different-sized photobleached areas ("beam-size" test) (Elson, 1985; Niv *et al.*, 1999). Two distinct areas were analyzed, in or outside cell-cell contacts (Figure 5A). The outside measurements were performed in the dorsal part of the plasma membrane (DPM). The linear relation observed between the characteristic diffusion time ($t_{1/2}$) and the illuminated area shows that N-cadherin in the plasma membrane moves by lateral diffusion (Figure 5B). Similar data were obtained at cell-cell contacts (Figure 6A).

The apparent D and M values of Ncad/GFP were first measured on confocal optical sections in the DPM by using identical sized bleach boxes. Disruption of lipid rafts or F-actin increased the diffusion rate of Ncad/GFP in the DPM by 2 two- and fourfold, respectively, but it did not modify the mobile pool of Ncad/GFP (Figure 5C). It has been shown that stable association of influenza hemagglutinin protein with an immobilized partner reduces its mobile fraction (Shvartsman *et al.*, 2003). For N-cadherin, because the M value is not affected, it seems to diffuse in the plane of the plasma membrane of C2C12 myoblasts without any stable association with lipid rafts or the F-actin cytoskeleton for the entire duration of the measurement. In contrast, these two structures decrease the lateral diffusion of N-cadherin, either by an indirect confinement effect or by a transient association with N-cadherin. Regardless, the F-actin cytoskeleton produces a higher constraint than the lipid rafts.

We then measured the D and M values of Ncad/GFP at cell-cell contact sites (Figure 6C). Unlike epithelial cells, myoblasts show only two distinct stages in cell-cell contact formation (Adams *et al.*, 1998). The first stage, called AJ1 (Figure 6C, a) corresponds to a cell-cell contact "in formation" and is often seen in subconfluent cells. The second stage, called AJ2, corresponds to an established cell-cell contact and is observed in fully contacting cells (Figure 6C, b). We found a twofold decrease in the lateral diffusion and the mobile fraction of Ncad/GFP at the AJ2 cell-cell contact (Figure 6C, c and d, compare the D and M values between the AJ1 and the AJ2 stages). To better illustrate the correlation between the degree of development of cell-cell contacts and the concomitant modifications in D and M, three images with their corresponding D and M values are shown in Figure 6D. These data indicate that half of the initially highly mobile pool of Ncad/GFP becomes immobilized during cell-cell contact establishment. To understand the molecular mechanisms involved in N-cadherin stabilization at cell contacts, we first analyzed the effect of both homophilic ligation and F-actin cytoskeleton, two known regulators of cadherin-mediated cell-cell adhesion (Volberg *et al.*, 1986; Adams *et al.*, 1996, 1998), on N-cadherin diffusion. Both the addition of EGTA, which chelates extracellular Ca^{2+} and perturbs homophilic interactions, and cytochalasin B (CY), which disrupts the F-actin cytoskeleton, to cell having established cell contacts, led to an increase in the mobile fraction and lateral mobility of Ncad/GFP (Figure 6C, c and d, compare AJ2 to AJ2/EGTA and AJ2/CY). We then analyzed the effect of lipid raft disruption on these two parameters. Interestingly, addition of CO to contacting cells induced an increase in both D and M of Ncad/GFP (compare AJ2 to AJ2/CO). Addition of cholesterol-containing medium brings back D and M at the AJ2 level (our unpublished data). Typical images of FRAP experiments from control AJ2 and CO-treated AJ2 cells are shown in Figure 6E. These data suggest that a pool of Ncad/GFP becomes immobilized during junction establishment. Homophilic cell-cell adhesion, F-actin cytoskeleton, and lipid rafts decrease the lateral diffusion and mobile fraction of N-cadherin at cell-cell contacts and thus participate to its immobilization during contact establishment.

Association of N-Cadherin to Lipid Rafts Requires Homophilic Binding and F-Actin Association

Formation of cadherin-dependent cell-cell adhesion requires Ca^{2+} to form homophilic interactions and the attachment of cadherin–catenin complexes to the F-actin cytoskeleton (Volberg *et al.*, 1986; Adams *et al.*, 1996, 1998). We studied whether Ca^{2+} chelation with EGTA or F-actin depolymerization has an effect on N-cadherin association to lipid rafts. We first analyzed the effect of these treatments on N-cadherin association to DRMs by using sucrose gradients. Both EGTA and cytochalasin B treatments strongly decreased N-cadherin association to DRMs (Figure 7A). Similar results have been obtained using cells cultured in Ca^{2+}-depleted medium (our unpublished data). In contrast, the amount of caveolin found in DRMs was not affected by these treatments. We then analyzed the localization of N-cadherin after extraction with cold 1% Triton X-100 before fixation in EGTA- and cytochalasin-treated cells. As shown in Figure 7B, EGTA and cytochalasin treatments perturbed N-cadherin localization at cell-cell contacts (a and c) and strongly
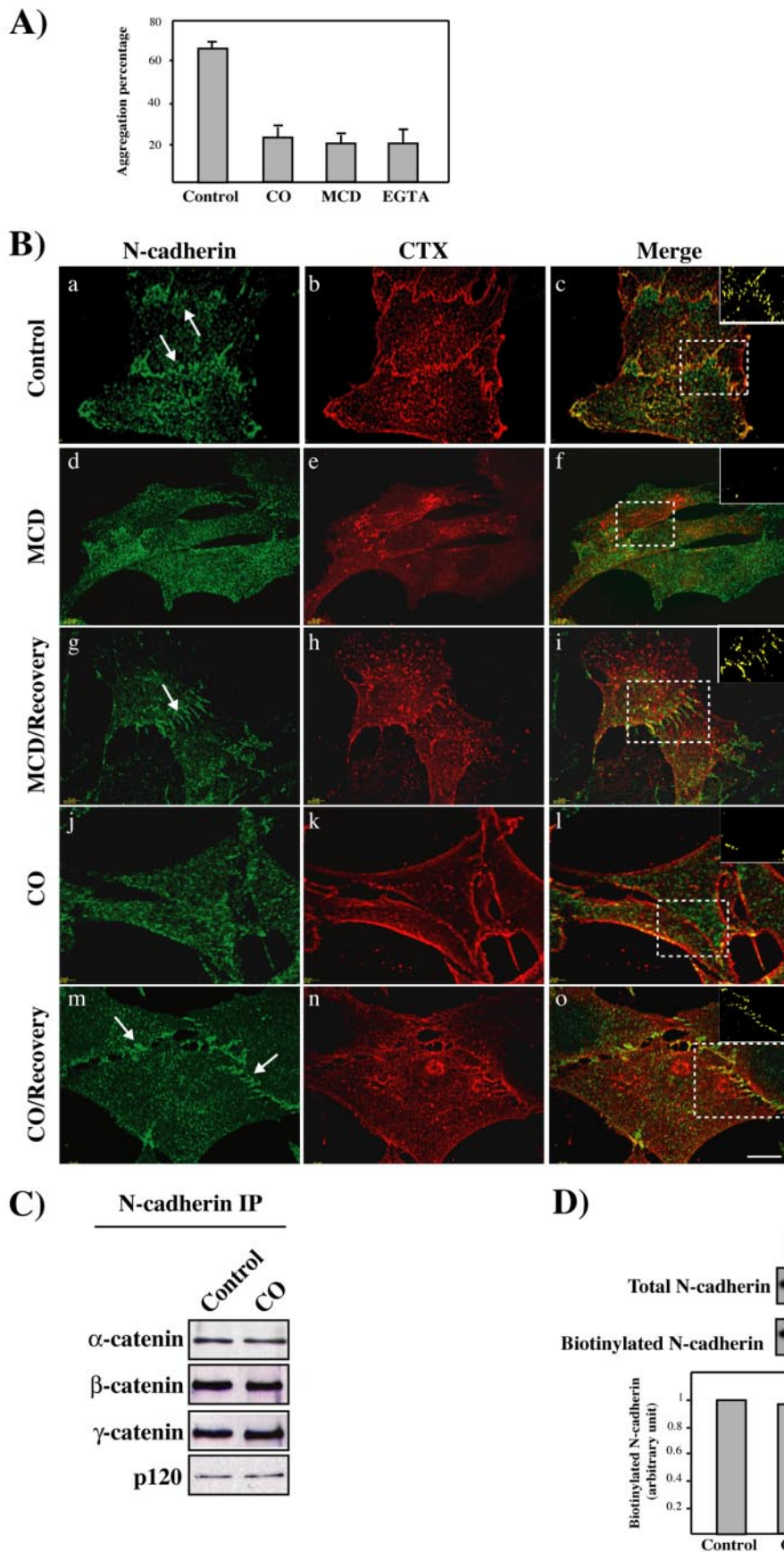
Figure 4. Disruption of lipid rafts and N-cadherin association at cell-cell contacts. (A) The graph shows the percentage of clustered cells from control, CO-, MCD-, or EGTA-treated C2C12 myoblasts 30 min after aggregation. (B) C2C12 myoblasts were treated with MCD or CO as indicated. Addition of cholesterol was performed after the first treatment. Cells were either stained for N-cadherin (a, d, g, j, and m) or GM1 distribution with CTX (b, e, h, k, and n). Deconvolved stacks of images were visualized using Imaris software. Arrows point to areas of N-cadherin localization at the cell-cell contacts. Merge images are shown in c, f, I, l, and o. The respective voxel colocalizations of N-cadherin with GM1 were obtained using the Imaris colocalization module and are shown in the insets of c, f, I, l, and o. Bar, 10 μm. (C) Cell lysates of C2C12 myoblasts treated with CO or controls were immunoprecipitated using an anti-N-cadherin antibody and immunoblotted for the presence of α-, β-, γ-, and p120 catenins. (D) Surface biotinylation of N-cadherin from control or CO-treated C2C12 myoblasts. The histogram represents the mean level of biotinylated N-cadherin normalized to the amount of total protein from three independent experiments.
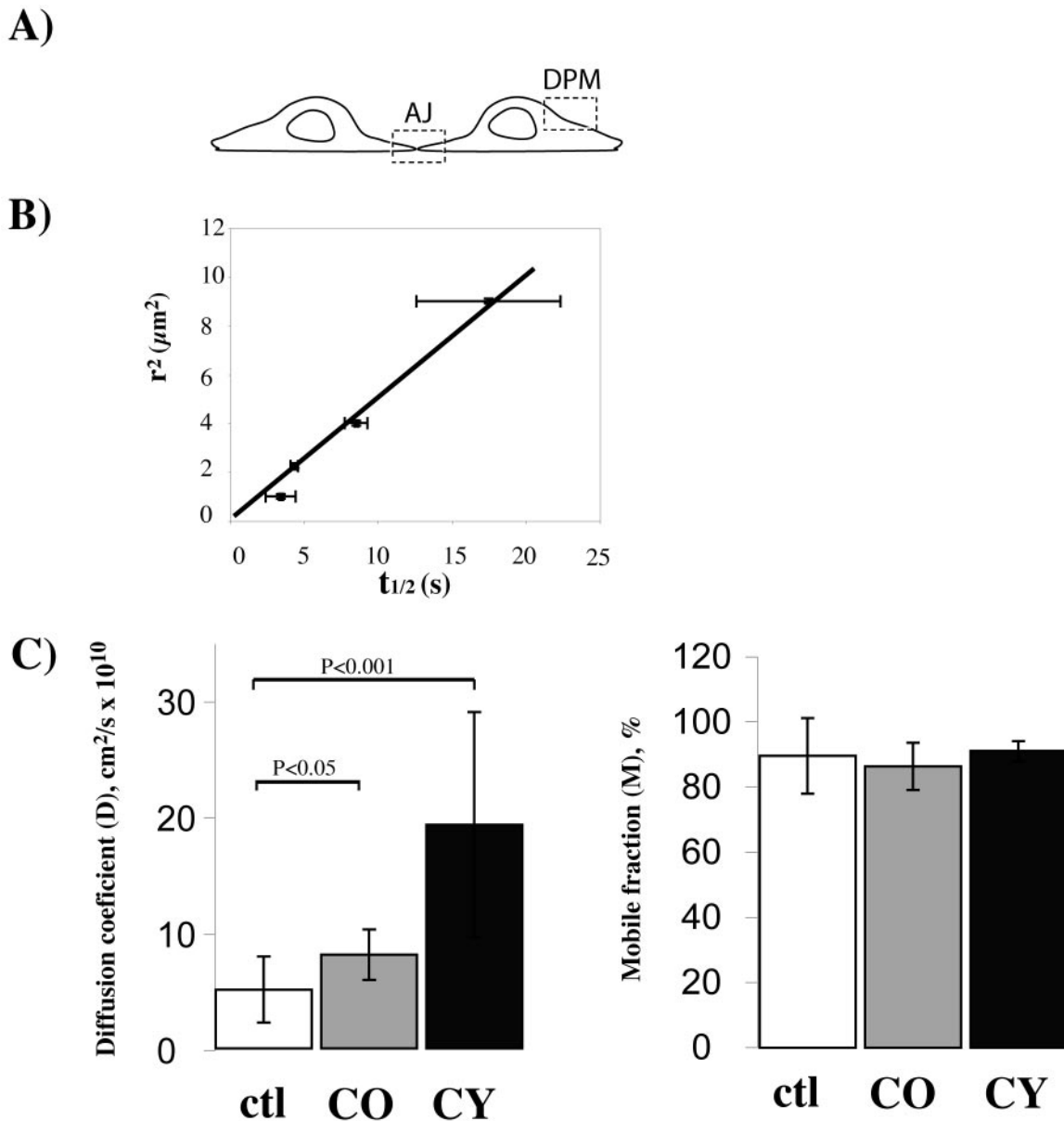
A)

B)

C)

Figure 5. Measurement of the mobile pool and lateral mobility of N-cadherin outside cell contacts. (A) Schematic visualization of two contacting cells showing the sites of measurement. Membrane not involved in cell-cell contact corresponds to the DPM. Membrane involved in cell-cell contact is the site of adherent junction (AJ) formation where Ncad/GFP accumulates. (B) Fluorescence half-recovery time of Ncad/GFP ($t_{1/2}$) measured at the DPM is proportional to the bleached area size. (C) Measure of D and M coefficients of Ncad/GFP in membrane not involved in cell-cell contact after destructuration of lipid rafts (by CO) and F-actin cytoskeleton (by CY). Each bar is the mean $\pm$ SEM of 15 measurements and statistical differences are indicated.

decreased the insoluble pool of N-cadherin located at these cell-cell contacts (b and d). These data indicate that homophilic interactions and the F-actin cytoskeleton participate in the association of N-cadherin with lipid rafts.

DISCUSSION

Our knowledge of the mechanisms and dynamics of cadherin-mediated adhesion remains fragmentary. It is known that the establishment of cell-cell contacts is initiated by the adhesive interactions of cadherin ectodomains on adjacent cells that may regulate the anchoring of cadherin–catenin complexes to the actin cytoskeleton (Adams *et al.*, 1998;

Lambert *et al.*, 2002). This association of the cytoplasmic domain of cadherins to actin filaments is in turn required for the adhesive function of the cadherin ectodomain (Nagafuchi and Takeichi, 1988). The plasma membrane organization might also participate in cadherin stabilization at cell-cell contact sites. To test this hypothesis, we first analyzed whether N-cadherin in myoblasts is associated with membrane compartments called lipid rafts. We took advantage of the insolubility of raft components in cool detergent to show that a pool of N-cadherin is present in these aggregates of sphingolipids and cholesterol. Cross-linking of the raft molecule cholera toxin, allowing raft detection by light microscopy (Harder *et al.*, 1998), confirmed that N-cadherin is
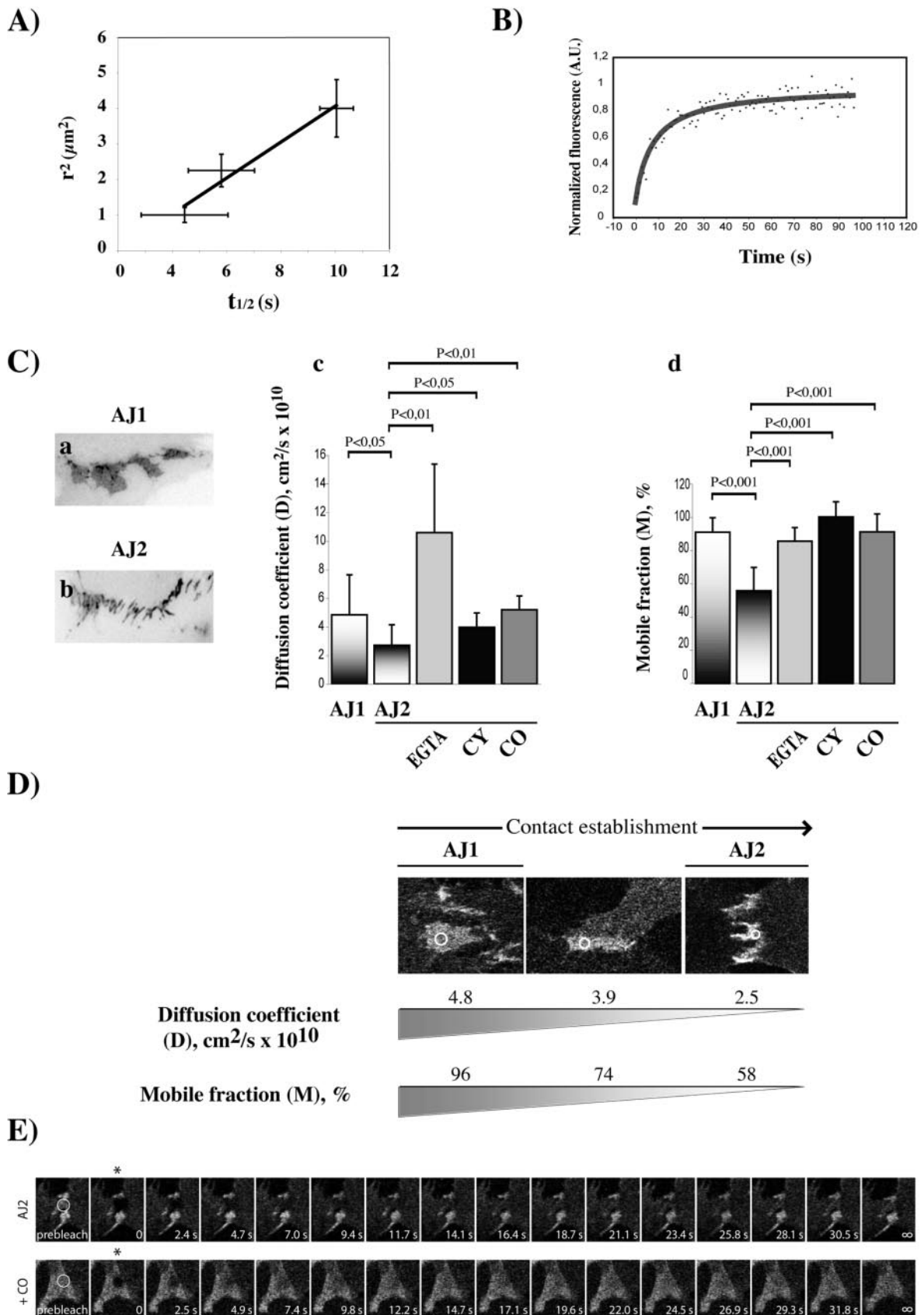
Figure 6.

A)

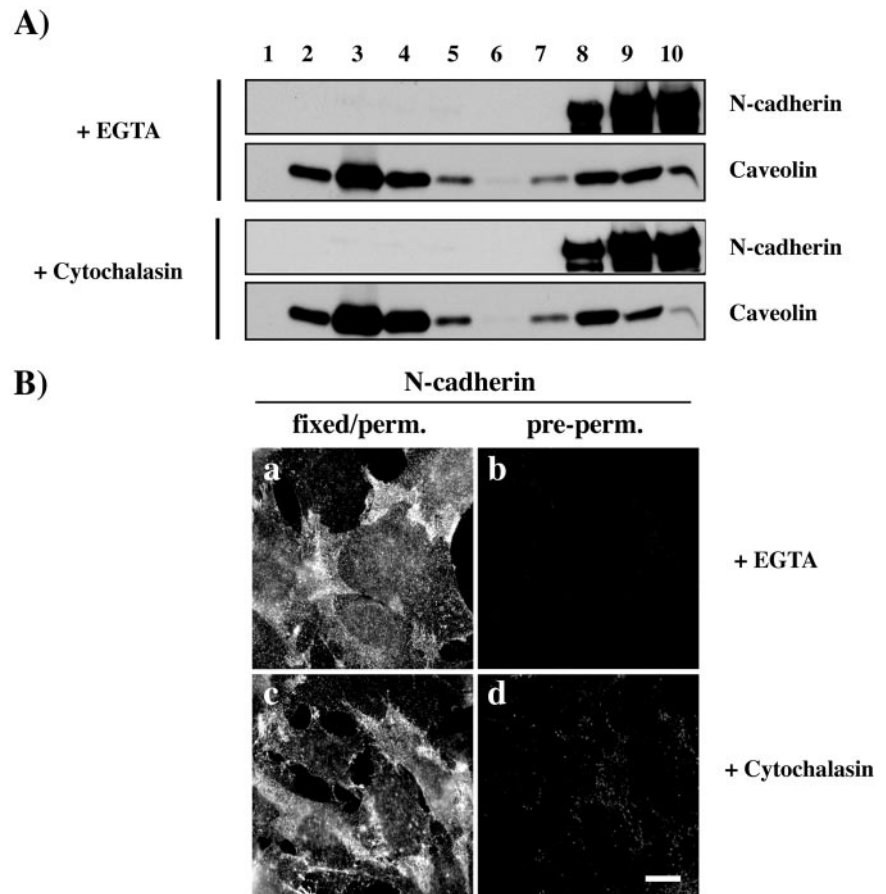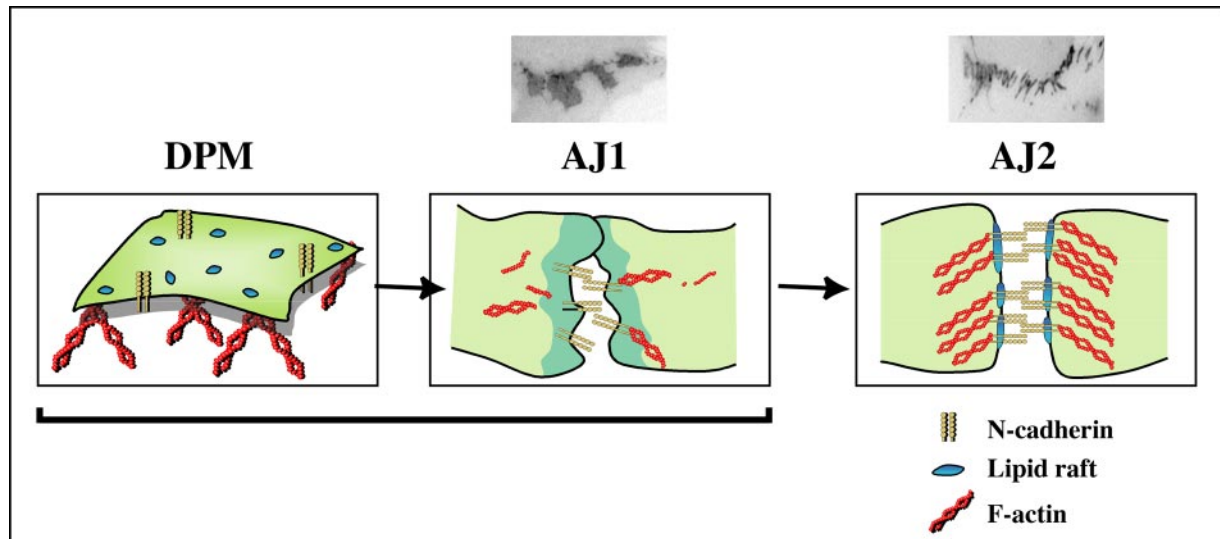
+ EGTA

+ Cytochalasin

B)

Figure 7. N-cadherin association to lipid rafts requires homophilic interactions and F-actin association. (A) C2C12 myoblasts treated with EGTA or cytochalasin were fractionated on sucrose gradients. Each fraction (30 μl) was analyzed for N-cadherin and caveolin distribution by immunoblotting. (B) C2C12 myoblasts treated with EGTA or cytochalasin were fixed either before (a) or after (b) extraction with cold 1% Triton X-100 and stained with an antibody against N-cadherin. Bar, 10 μm.

Figure 6 (facing page). Lipid raft disruption increases the mobile pool and lateral mobility of N-cadherin at cell-cell contact sites. (A) Fluorescence half-recovery time of Ncad/GFP ($t_{1/2}$) measured at the cell-cell contact is proportional to the bleached area size. (B) Shown are the first 90 s of photobleach recovery data of Ncad/GFP in an AJ1 cell contact. The solid line represents the best fit to the lateral diffusion equation as described in the material and methods. (C) Effect of disruption of Ca^{2+}-dependent homophilic adhesion (by EGTA), F-actin (by CY), and LR (by CO) on the D and M coefficients of Ncad/GFP in membranes involved in cell-cell contacts. AJ1 represents a cell-cell contact in formation (a). AJ2 corresponds to an established cell-cell contact (b). Significance (by paired Student's t test) is shown on the graph. (D) Visualization of the decrease in the D and M values with the development of cell-cell contacts. Three representative images of Ncad/GFP organization during cell contact establishment with the corresponding D and M values are shown. Circles show the selected area for fluorescence measurements. (E) Shown are typical images of a FRAP experiment. Fluorescence of selected areas (circles) of N-cadherin-dependent cell-cell contacts of the AJ2 type from control or CO-treated were photobleached (the first image recorded after bleaching is marked by an asterisk), and fluorescence recovery was measured at the indicated time points.

present in these structures. In cerebellar granule cells, N-cadherin also has been detected in lipid rafts (Nakai 2002). However, the localization of this association was difficult to assess. Indeed, the presumed size of rafts is <100 nm, falling below the resolution of light microscopy techniques. Nevertheless, our light microscopy data revealed a strong colocalization of N-cadherin with lipid raft molecules at cell-cell

contacts. The demonstration that this pool of N-cadherin is associated with lipid rafts came from the observation of its insolubility in the nonionic detergent Triton X-100 (Simons and Ikonen, 1997). Recently, Kusumi and coworkers have emphasized the importance of clearly distinguishing between two types of rafts: the small ones present in resting cells and the receptor-cluster rafts induced by ligariding and cross-linking of raft-preferring molecules according to the lipid shell model (Anderson and Jacobson, 2002; Kusumi *et al.*, 2004). Therefore, N-cadherin at a cell-cell contact might generate this latter type of raft, which is visible by light microscopy.

Formation of adherens junction is a multistep process that includes cadherin association with catenins, delivery of cadherin–catenin complexes to the plasma membrane, and lateral diffusion in the plasma membrane toward cell-cell contact sites. It was demonstrated previously that N-cadherin is transported from the Golgi to the plasma membrane through a microtubule-, kinesin-dependent mechanism (Mary *et al.*, 2002; Chen *et al.*, 2003). But once at the dorsal cell surface, N-cadherin diffusion in the plasma membrane might be required for its assembly at the cell-cell contact. Various reports have shown that E-cadherin and N-cadherin are diffusing within the membrane (Kusumi *et al.*, 1993; Sako *et al.*, 1998; Lambert *et al.*, 2002). Therefore, the mechanism that regulates the movement of cadherin on the cell surface inside and outside the cell-cell contact is important to understand. Using FRAP, we have analyzed the movement of N-cadherin in these two distinct places of the plasma membrane (Figure 8). We present the first analysis of the behavior

	DPM		AJ1		AJ2
Diffusion coefficient (D) (cm≤/s x 10^{10})	4.3 ± 2,4	=	4.8 ± 2,8	>	2.7 ± 1,4
Mobile fraction (M) (%)	89 ± 12	=	91 ± 9	>	56 ± 14

Figure 8. Model for the role of lipid rafts in the dynamics of N-cadherin–mediated junction assembly. In the dorsal cell surface, N-cadherin diffusion is indirectly regulated by lipid rafts and the F-actin cytoskeleton (D is affected by drugs which disrupt these structures). The absence of any effect on the size of the mobile fraction (M exclude a direct association of N-cadherin with these structures at the DPM). The lateral diffusion coefficient and mobile pool of N-cadherin is similar in the DPM and in AJ1-type cell-cell contacts. During the establishment of cell-cell contacts (transition from AJ1 to AJ2), a pool of N-cadherin molecules become immobilized through the formation of homophilic interaction and its association with the lipid rafts and the F-actin cytoskeleton (both D and M are modified). D values are in the range expected for a transmembrane protein.

of cadherin outside cell-cell contacts without homotypic activation of the molecule. Previous studies only analyzed the translational movement of E- or N-cadherin in conditions mimicking cadherin-mediated adhesion (Kusumi *et al.*, 1993; Sako *et al.*, 1998; Lambert *et al.*, 2002). We find that the diffusion of N-cadherin in the dorsal part of the plasma membrane outside cell-cell contacts is indirectly regulated by the F-actin cytoskeleton. In other words, N-cadherin is not tethered by these structures, but its mobility is decreased by the membrane skeleton fence. This is in agreement with the membrane skeleton fence model proposed for E-cadherin (Sako *et al.*, 1998). Lipid rafts in the plasma membrane that are outside cell-cell contacts also decrease the mobility of N-cadherin. This is not due to a direct association of N-cadherin: our findings that disruption of the F-actin cytoskeleton or lipid rafts did not change the size of the immobile fractions allowed us to exclude the possibility that there was a direct association of N-cadherin with these two structures at the dorsal plasma membrane, as also shown by others (Shvartsman *et al.*, 2003; Kenworthy *et al.*, 2004). The constraint induce by F-actin is higher than the one induced by lipid rafts. This is in agreement with data showing that raft association is not the major determinant of the diffusional mobility of plasma membrane proteins under steady-state condition (Kenworthy *et al.*, 2004). The effect of lipid raft disruption on the diffusional mobility of N-cadherin might be explained by the structural organization of these lipid rafts that could act as a brake in the motion of plasma

membrane proteins that have to cross or bypass these structures. Lipid rafts are enriched in cholesterol, shingolipids with their usually saturated fatty acids, and saturated glycerophospholipids. The structure of their hydrophobic moieties allows them to be packed more tightly than unsaturated lipids, establishing a more ordered state, called the liquid-ordered (l_0) phase interspersed in the continuous liquid-disorder (l_d) phase.

This work is, to our knowledge, the first analysis of the dynamic of N-cadherin diffusional mobility during endogenous cell-cell contact formation. Indeed, previous studies have reproduced artificial cell-cell contacts by adding beads bound to either cadherin molecules or anti-cadherin antibodies (Sako *et al.*, 1998; Lambert *et al.*, 2002). The establishment of cell-cell contacts is characterized by a decrease in N-cadherin mobility and the immobilization of a pool of protein. The D and M values are similar at the dorsal plasma membrane and in AJ1 cell-cell contact but are significantly decreased in the AJ2 stage (Figure 8). Together, these data support a model in which N-cadherin molecules are free to diffuse in the dorsal plasma membrane and at early stage of cell-cell contact (AJ1) before their immobilization at the time when cell-cell contact is established (AJ2). The search for factors regulating the stabilization process prompted us to test the involvement of two known and one unexpected regulators of cell-cell contact formation, homophilic interaction and F-actin and lipid rafts, respectively. Homophilic binding between extracellular domains of N-cadherin and

the F-actin cytoskeleton participates in N-cadherin stabilization at cell-cell contacts. Homophilic binding has a prominent effect on the lateral diffusion of N-cadherin, whereas anchoring to the F-actin cytoskeleton is clearly responsible for its immobilization at cell-cell contacts. This is in agreement with the current model in which a highly mobile pool of cadherin molecules becomes immobilized as a result of homophilic ligand-triggered recruitment before anchoring to the F-actin cytoskeleton (Adams *et al.*, 1998; Lambert *et al.*, 2002). In addition, lipid raft association at cell-cell contacts specifically decreases N-cadherin lateral diffusion and the size of its immobile fraction. This is the first demonstration that lipid rafts play a role in N-cadherin stabilization at the cell junction. Several models can be proposed. First, lipid rafts preexist at the cell-cell contacts. N-cadherin diffusing in the plasma membrane is trapped and immobilized in these microdomains. Second, lipid raft formation at cell-cell contacts is a consequence of N-cadherin oligomerization and homotypic interactions. Each N-cadherin molecule might be surrounded by a lipid shell and the accumulation of N-cadherin at the cell-cell contacts would lead to the formation of this "lipid raft zone" or a transient confinement zone in which the diffusion of N-cadherin is slowed (Anderson and Jacobson, 2002). Whether rafts and F-actin association act synergistically or sequentially remains to be determined. Anchoring of N-cadherin along the actin-based membrane skeleton mesh might act as rows of pickets that temporarily confine phospholipids as proposed in the anchored protein picket model (Kusumi *et al.*, 2004). Alternatively, sufficient N-cadherin immobilization might allow its interaction with the F-actin cytoskeleton to form a cell-cell adhesion structure. Our data showing that F-actin disruption perturbs N-cadherin association with lipid rafts argues for the first hypothesis. Thus, N-cadherin-induced raft formation might play an important role in organizing signal transduction pathways in this specific area of the membrane.

There is a growing body of evidence that multiple molecular interactions required for cells to process information received from their environment occurs in specific membrane domains such as caveolae, focal adhesion sites, or sites of cell-cell contact. Further studies are necessary to analyze the functional role of N-cadherin association with lipid rafts in cell signaling.

REFERENCES

Adams, C. L., Chen, Y. T., Smith, S. J., and Nelson, W. J. (1998). Mechanisms of epithelial cell-cell adhesion and cell compaction revealed by high-resolution tracking of E-cadherin-green fluorescent protein. J. Cell Biol. *142*, 1105–1119.

Adams, C. L., Nelson, W. J., and Smith, S. J. (1996). Quantitative analysis of cadherin-catenin-actin reorganization during development of cell-cell adhesion. J. Cell Biol. *135*, 1899–1911.

Anderson, R. G., and Jacobson, K. (2002). A role for lipid shells in targeting proteins to caveolae, rafts, and other lipid domains. Science *296*, 1821–1825.

Axelrod, D., Koppel, D. E., Schlessinger, J., Elson, E., and Webb, W. W. (1976). Mobility measurement by analysis of fluorescence photobleaching recovery kinetics. Biophys. J. *16*, 1055–1069.

Charrasse, S., Meriane, M., Comunale, F., Blangy, A., and Gauthier-Rouviere, C. (2002). N-Cadherin-dependent cell-cell contact regulates Rho GTPases and beta-catenin localization in mouse C2C12 myoblasts. J. Cell Biol. *158*, 953–965.

Chen, X., Kojima, S., Borisy, G. G., and Green, K. J. (2003). p120 catenin associates with kinesin and facilitates the transport of cadherin-catenin complexes to intercellular junctions. J. Cell Biol. *163*, 547–557.

Chen, Y. T., Stewart, D. B., and Nelson, W. J. (1999). Coupling assembly of the E-cadherin/beta-catenin complex to efficient endoplasmic reticulum exit and basal-lateral membrane targeting of E-cadherin in polarized MDCK cells. J. Cell Biol. *144*, 687–699.

Drevot, P., Langlet, C., Guo, X. J., Bernard, A. M., Colard, O., Chauvin, J. P., Lasserre, R., and He, H. T. (2002). TCR signal initiation machinery is preassembled and activated in a subset of membrane rafts. EMBO J. *21*, 1899–1908.

Elson, E. L. (1985). Fluorescence correlation spectroscopy and photobleaching recovery. Annu. Rev. Phys. Chem. *36*, 379–406.

Gauthier-Rouviere, C., Vignal, E., Meriane, M., Roux, P., Montcourier, P., and Fort, P. (1998). RhoG GTPase controls a pathway that independently activates Rac1 and Cdc42Hs. Mol. Biol. Cell *9*, 1379–1394.

Gkantiragas, I., Brugger, B., Stuven, E., Kaloyanova, D., Li, X. Y., Lohr, K., Lottspeich, F., Wieland, F. T., and Helms, J. B. (2001). Sphingomyelin-enriched microdomains at the Golgi complex. Mol. Biol. Cell *12*, 1819–1833.

Harder, T., Scheiffele, P., Verkade, P., and Simons, K. (1998). Lipid domain structure of the plasma membrane revealed by patching of membrane components. J. Cell Biol. *141*, 929–942.

Harder, T., and Simons, K. (1997). Caveolae, DIGs, and the dynamics of sphingolipid-cholesterol microdomains. Curr. Opin. Cell Biol. *9*, 534–542.

Ilangumaran, S., and Hoessli, D. C. (1998). Effects of cholesterol depletion by cyclodextrin on the sphingolipid microdomains of the plasma membrane. Biochem. J. *335*, 433–440.

Iwabuchi, K., Handa, K., and Hakomori, S. (1998). Separation of "glycosphingolipid signaling domain" from caveolin-containing membrane fraction in mouse melanoma B16 cells and its role in cell adhesion coupled with signaling. J. Biol. Chem. *273*, 33766–33773.

Jacobson, K., Sheets, E. D., and Simson, R. (1995). Revisiting the fluid mosaic model of membranes. Science *268*, 1441–1442.

Janes, P. W., Ley, S. C., and Magee, A. I. (1999). Aggregation of lipid rafts accompanies signaling via the T cell antigen receptor. J. Cell Biol. *147*, 447–461.

Kenworthy, A. K., Nichols, B. J., Remmert, C. L., Hendrix, G. M., Kumar, M., Zimmerberg, J., and Lippincott-Schwartz, J. (2004). Dynamics of putative raft-associated proteins at the cell surface. J. Cell Biol. *165*, 735–746.

Kurzchalia, T. V., and Parton, R. G. (1999). Membrane microdomains and caveolae. Curr. Opin. Cell Biol. *11*, 424–431.

Kusumi, A., Koyama-Honda, I., and Suzuki, K. (2004). Molecular dynamics and interactions for creation of stimulation-induced stabilized rafts from small unstable steady-state rafts. Traffic *5*, 213–230.

Kusumi, A., Sako, Y., and Yamamoto, M. (1993). Confined lateral diffusion of membrane receptors as studied by single particle tracking (nanovid microscopy). Effects of calcium-induced differentiation in cultured epithelial cells. Biophys. J. *65*, 2021–2040.

Lambert, M., Choquet, D., and Mege, R. M. (2002). Dynamics of ligand-induced, Rac1-dependent anchoring of cadherins to the actin cytoskeleton. J. Cell Biol. *157*, 469–479.

Le, T. L., Yap, A. S., and Stow, J. L. (1999). Recycling of E-cadherin: a potential mechanism for regulating cadherin dynamics. J. Cell Biol. *146*, 219–232.

Mary, S., Charrasse, S., Meriane, M., Comunale, F., Travo, P., Blangy, A., and Gauthier-Rouviere, C. (2002). Biogenesis of N-cadherin-dependent cell-cell contacts in living fibroblasts is a microtubule-dependent kinesin-driven mechanism. Mol. Biol. Cell *13*, 285–301.

Nagafuchi, A., and Takeichi, M. (1988). Cell binding function of E-cadherin is regulated by the cytoplasmic domain. EMBO. J. *7*, 3679–3684.

Niethammer, P., Delling, M., Sytnyk, V., Dityatev, A., Fukami, K., and Schachner, M. (2002). Cosignaling of NCAM via lipid rafts and the FGF receptor is required for neuritogenesis. J. Cell Biol. *157*, 521–532.

Niv, H., Gutman, O., Henis, Y. I., and Kloog, Y. (1999). Membrane interactions of a constitutively active GFP-Ki-Ras 4B and their role in signaling. Evidence from lateral mobility studies. J. Biol. Chem. *274*, 1606–1613.

Roepstorff, K., Thomsen, P., Sandvig, K., and van Deurs, B. (2002). Sequestration of epidermal growth factor receptors in non-caveolar lipid rafts inhibits ligand binding. J. Biol. Chem. *277*, 18954–18960.

Sako, Y., Nagafuchi, A., Tsukita, S., Takeichi, M., and Kusumi, A. (1998). Cytoplasmic regulation of the movement of E-cadherin on the free cell surface

as studied by optical tweezers and single particle tracking: corralling and tethering by the membrane skeleton. J. Cell Biol. *140*, 1227–1240.

Shvartsman, D. E., Kotler, M., Tall, R. D., Roth, M. G., and Henis, Y. I. (2003). Differently anchored influenza hemagglutinin mutants display distinct interaction dynamics with mutual rafts. J. Cell Biol. *163*, 879–888.

Simons, K., and Ikonen, E. (1997). Functional rafts in cell membranes. Nature *387*, 569–572.

Simons, K., and Toomre, D. (2000). Lipid rafts and signal transduction. Nat. Rev. Mol. Cell. Biol. *1*, 31–39.

Smart, E. J., and Anderson, R. G. (2002). Alterations in membrane cholesterol that affect structure and function of caveolae. Methods Enzymol. *353*, 131–139.

Volberg, T., Geiger, B., Kartenbeck, J., and Franke, W. W. (1986). Changes in membrane-microfilament interaction in intercellular adherens junctions upon removal of extracellular Ca2+ ions. J. Cell Biol. *102*, 1832–1842.

Wahl, J. K., 3rd, Kim, Y. J., Cullen, J. M., Johnson, K. R., and Wheelock, M. J. (2003). N-cadherin-catenin complexes form prior to cleavage of the proregion and transport to the plasma membrane. J. Biol. Chem. *278*, 17269–17276.